

Analysis of Print Gloss with a Calibrated Microgoniophotometer

J. S. Arney[▲] and David Nilosek

Center for Imaging Science, Rochester Institute of Technology,

54 Lomb Memorial Drive, Rochester, New York 14623

E-mail: arney@cis.rit

Abstract. A procedure for the calibration of a microgoniophotometer is described that enables the analysis of gloss data in terms of the underlying optical properties of the glossy material. Calibration studies are described and calibration procedures are presented, along with a discussion of accuracy and precision characteristics of the current instrument. Examples of analytical applications are described in which the utility of the calibrated device is demonstrated. These examples demonstrate analytical protocols capable of distinguishing between the effects of two key optical constants (n and κ) and the angular distribution of surface facets. In addition, by calibrating the device in separate red, green, and blue bands of light, measurements can provide information relevant to chromatic changes in optical constants and the effects of sublayer specular contributions to gloss. This work is intended provide a tool for imaging scientists concerned with the effects of material properties on the gloss of printed materials. Future work will address the instrumental measurement of appearance attributes of gloss. © 2007 Society for Imaging Science and Technology. [DOI: 10.2352/J.ImagingSci.Technol.(2007)51:6(509)]

INTRODUCTION

The term “gloss” is used in this article to mean the appearance properties of materials, as described by Hunter and Harlod.¹ In other words, gloss is not a material property but a group of visual effects produced by underlying material properties. The underlying material properties thought to contribute to gloss include the refractive index, the absorption coefficient, and the distribution of surface facet angles. An instrument designed to measure gloss might be designed to correlate with the visual features of gloss, or it might be designed to measure the underlying material properties that govern gloss. Recent work in this laboratory has led to instrumentation that we believe has the potential to serve both needs, and thus provide information about how control of basic material properties will be manifested in the appearance of gloss.^{2–5} This article describes the calibration of a microgoniophotometer to measure material properties, and future articles will describe work on calibration of the instrument to visual attributes.

The term “calibration”, as used in the current work, is meant to describe a process of canceling out the properties of the instrument so that the measurement provides infor-

mation only about the sample material under analysis. Traditional gloss meters have not achieved this kind of calibration. The calibration protocol for a traditional gloss meter, which involves a black glass reference of known refractive index, can result in very repeatable measurements. However, the method of calibrating a gloss meter does not completely cancel differences between instruments, and so measurements with one calibrated gloss meter may not agree with another calibrated gloss meter measuring the same material and calibrated to the same black glass standard.⁶ As described next, the microgoniophotometer can be calibrated to yield the actual specular reflectance factor, ρ , of the material under analysis. Moreover, application of appropriate experimental protocols for measuring ρ can distinguish between surface topographic effects and the complex index of refraction of the material. As will be demonstrated, measurements made with this instrument can provide guidance to the imaging scientist about the material properties underlying gloss appearance characteristics.

CONFIGURATION OF THE MICROGONIOPHOTOMETER

Figure 1 is a schematic illustration of the microgoniophotometer used in the current work. Details of the instrument are described elsewhere,^{2–5} and only a summary is given here. The printed sample is wrapped around a

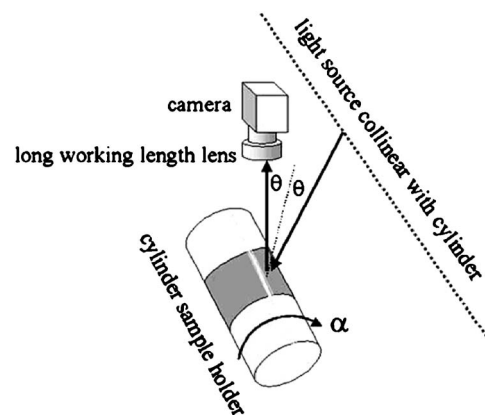


Figure 1. Schematic diagram of the instrument with specular angle = 20° . The cylinder diameter is 20 mm, and the camera and illumination distances are sufficiently long to minimize parallax.

[▲]IS&T Member

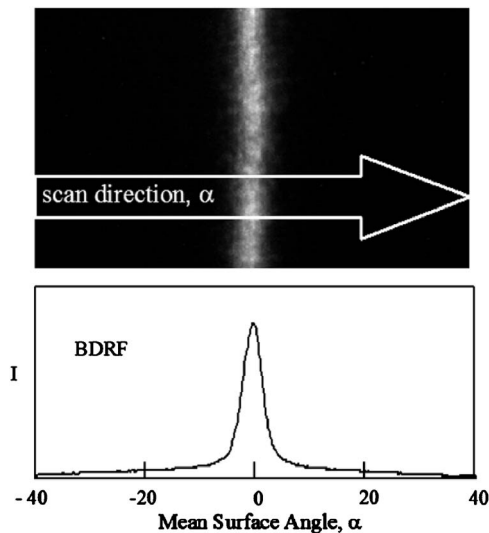


Figure 2. Illustration of an image and a BRDF from the device shown in Fig. 1. The scan direction covers 5 mm of the sample.

cylinder and illuminated with a line source that is collinear with the cylinder. A camera captures an image of the sample. The camera uses a lens with a long working distance so that parallax from one side of the sample to the other can be ignored. The line light source is sufficiently long and sufficiently far from the cylinder to approximate an infinitely long source at infinity. The light from the source is linearly polarized, and a second polarizer is used as an analyzer in front of the camera lens. Images are captured with both parallel and crossed polarizers, and a difference image is produced. The difference image contains only that light which maintains polarization when it is reflected. The bulk scattered light is randomly polarized and thereby eliminated from the measurement.

An illustration of an image captured with this goniophotometer is shown in Figure 2. The specular band is clearly visible, and its angular distribution is calculated from the known geometry of the cylinder. A horizontal scan of this image produces a type of bidirectional reflectance distribution function (BRDF). The specular lobe is centered at $\alpha=0$, where α is the mean surface angle of the sample.

CALIBRATION OF THE MICROGONIOPHOTOMETER

In order to calibrate the microgoniophotometer, it is useful to consider a mechanistic model for the way light is reflected from materials and detected by the instrument. The specular reflection of light from printed surfaces and substrates has been shown to be well described by a microfacet model.⁶⁻⁹ Each microfacet is tilted at some angle, α , relative to the mean surface. If the sample is tilted to an angle $-\alpha$, as illustrated in Figure 3, the microfacet is at exactly the correct orientation to reflect light into the detector. The microgoniophotometer in Fig. 1 operates exactly as shown in Fig. 3, with many different surface angles, α , presented to the detector simultaneously since the sample is wrapped around a cylinder.

A complete BRDF analysis would measure the specular lobe in both orthogonal directions α and β . However, the

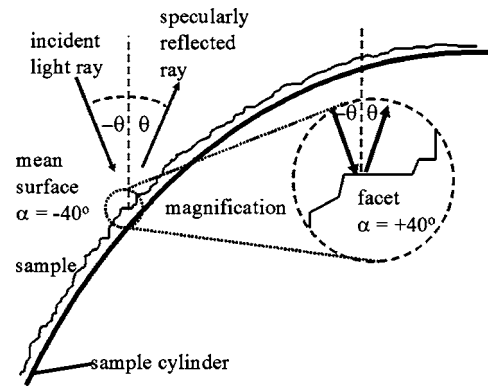


Figure 3. Magnified view of a section of the cylinder microgoniophotometer illustrates that the instrument measures light as a function of sample angle, α . Magnification to show individual facets illustrates that specular light is always detected at a constant Fresnel angle, θ , regardless of the sample angle, α .

instrument described in Fig. 1 uses an approximation of an infinitely long light source. As described previously, this averages the specular lobe in the β direction.^{2,4-6} As a result, one would expect the area under the BRDF measured by the cylinder microgoniophotometer to be directly proportional to the total amount of specular light reflected from the surface.

It should be pointed out that the experimental approach of Fig. 1 provides information about specular light reflected in only the α direction. This is not meant to imply that specular properties are the same in the α, β directions. Rather, it is an experimental tradeoff in favor of simplicity and convenience. Anisotropic behavior can be explored by measuring a sample mounted on the cylinder at different orientations or by using a more conventional goniophotometer. While anisotropic behavior is important in most printed images, it is not addressed in the current work.

The facet model of the cylinder microgoniophotometer suggests that calibration can be achieved by making measurements of the BRDF area relative to the BRDF area for a reference material of a known Fresnel reflectance factor. This is shown in Eq. (1), where A and A_{ref} are the measured BRDF areas of the sample and the reference, ρ_{ref} is Fresnel reflectance factor of the reference, and ρ is the reflectance factor of the sample:

$$\rho = \rho_{\text{ref}} \frac{A}{A_{\text{ref}}} \quad (1)$$

The reference material chosen for this instrument was a sheet of polyvinyl acetate. The optical constants, n and κ , of polyvinyl acetate and other common materials examined in this project are shown in Table I.¹⁰⁻¹² Values of the Fresnel specular reflectance, ρ (literature), were calculated from n and κ by applying Fresnel's laws,¹⁰ and these values are also shown in Table I. The final column of Table I shows values of ρ measured by the microgoniophotometer, as just described. The liquid samples were measured by wrapping a filter paper around the instrument cylinder and soaking the paper with the liquid.

Table I. Optical properties^a of materials used in this project.

Material	n	κ	ρ (literature)	ρ (measured)
Water	1.33	0	0.020	0.020
Teflon	1.36	0	0.023	0.035
PvOAc (reference)	1.49	0	0.036	\equiv 0.036
Olive oil	1.47	0	0.039	0.039
Nylon	1.53	0	0.044	0.041
Nylon, black	—	—	—	0.041
Polycarbonate	1.585	0	0.051	0.054
Stainless steel	2.49	1.38	0.58	0.051
Aluminum	1.0	6.0	0.90	0.87

^aFrom Refs. 10–12.

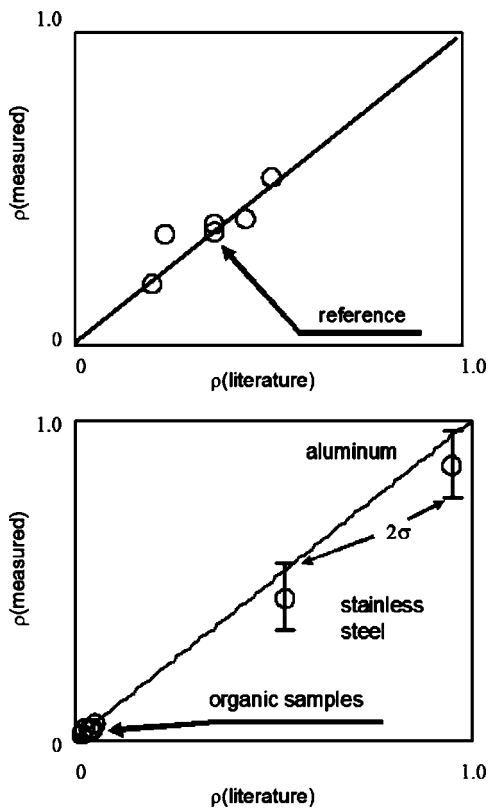


Figure 4. Correlation analysis of the Fresnel reflectance values ρ (measured) vs the literature values from Table I.

Figure 4 shows the relationship between the experimentally measured values of ρ and the ρ values from the literature. It is evident that the microgoniophotometer can be calibrated to provide an accurate measure of the specular reflectance of materials over a very wide range of optical properties.

It is interesting to note that the measured value of ρ for both the nylon and the black nylon samples are the same within experimental error. This seems to suggest that the optical constant $\kappa=0$ for the black nylon as well as for the ordinary nylon. The black nylon certainly has a black colorant in it with a nonzero extinction coefficient, $\epsilon > 0$, so

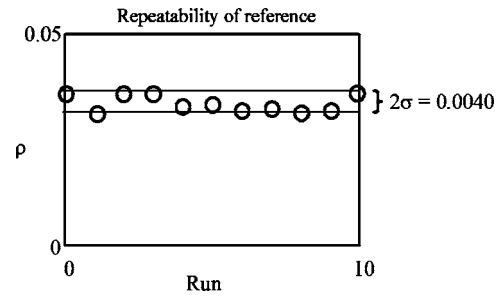


Figure 5. Test of precision for the measurement of the reference polyvinyl acetate. Eleven experimental estimates were made of ρ for the polyvinyl acetate.

the conclusion seems to be that the extinction coefficient ϵ must not be sufficiently large to make κ significantly greater than zero. The role of complex indexes of refraction in controlling ρ will be examined in more detail later in this article.

THE PRECISION OF THE MICROGONIOPHOTOMETER

In order to explore the potential level of precision of the microgoniophotometric analysis, the area of the BRDF for a sample of polyvinyl acetate was measured multiple times. Between each measurement, the sample was removed from the instrument and the instrument was shut down and restarted. A total of 11 measurements were made, and the area was used as an estimate of A_{ref} in Eq. (1). Then, each individual area was converted to an estimate of ρ using the average A_{ref} . The results, shown in Figure 5, indicate that the analysis is capable of two significant figure precision for the estimation of ρ .

The precision characteristics of the analysis were further explored by altering the surface roughness of some of the samples. The facet theory of gloss suggests that the area of the BRDF is independent of the shape of the BRDF. The shape of the BRDF, according to recent work,² is a measure of, and only of, the probability density function for the distribution of the facet angles. To determine if ρ is indeed independent of the BRDF shape, the surface roughness of several of the materials in this study were altered by sanding with polishing type sandpapers of grits ranging from 1500 to 6000. No attempt was made to control the sanding process in any repeatable fashion. The intent was simply to make changes in the surface topography and then to measure the changed samples. The results, shown in Figure 6, show very little correlation between BRDF area (expressed as ρ) and the width of the BRDF. However, some samples did seem to vary in reflectance as the BRDF width increased.

Some insight into why the experimental estimate of ρ may vary with the BRDF width is suggested in the raw data shown in Figure 7. The BRDF must be integrated to produce an estimate of reflectance factor, ρ . Sanding with various grits of sandpaper widened the BRDF curves. Integration of bell shaped curves with long tails involves making a decision about when the tail reaches zero, relative to experimental error, and this decision can have a significant influence on the estimated value of the area, and thus on ρ . The authors

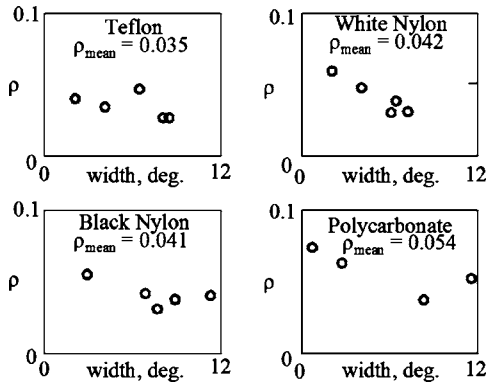


Figure 6. Experimental measurements of area of the BRDF, expressed as a reflectance factor, ρ , vs the width in degrees of the BRDF.

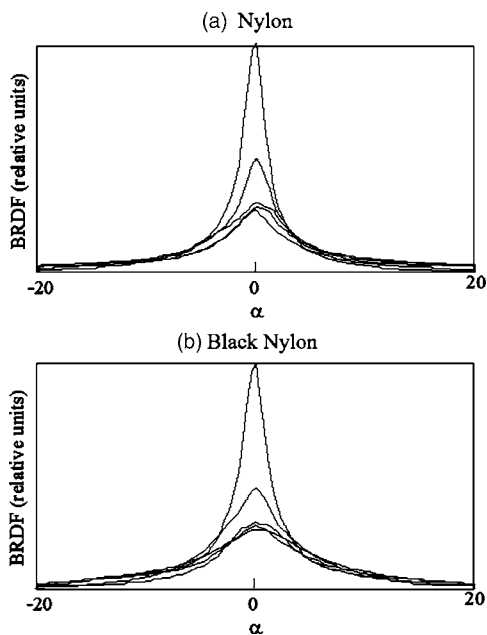


Figure 7. BRDF for (A) nylon and (B) black nylon for samples altered by different grits of sand paper.

would like to suggest that the apparent variation in ρ with width indicated by some of the samples in Fig. 6 is an artifact of the experimental difficulty in integrating the BRDF, and that the difficulty may be exacerbated by the introduction of extreme angles, α , in some of the facets by rougher types of sandpaper.

DIFFERENCES BETWEEN INKS

Different inks show different specular reflection characteristics. Two different black toners printed with two different printers are illustrated in Figure 8. The shapes of the two BRDF are very nearly the same, but the areas are significantly different. According to the facet theory, this can occur only if the optical constants of the two black toners are different. In order to examine this difference further, a series of measurements of ρ were made at different Fresnel angles, θ .

As illustrated in Fig. 3, the measurement of the BRDF, and therefore of ρ , is made at a single fixed value of θ . The

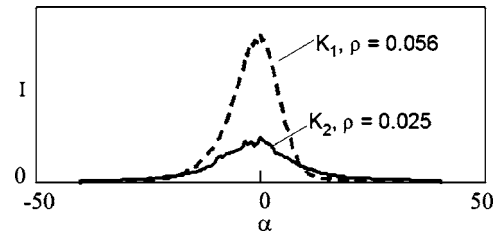


Figure 8. Black toner samples K_1 and K_2 from two different electrophotographic printers.

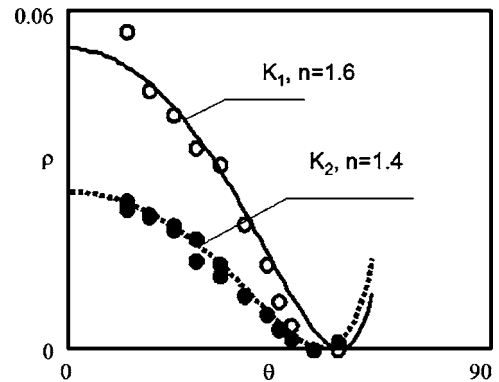


Figure 9. Black toner samples K_1 and K_2 from two different electrophotographic printers measured with linear polarized light in the p orientation. Fresnel's law is modeled in both cases with $\kappa=0$.

value of θ is the so-called gloss angle and can be selected in the microgoniophotometer. Values of ρ were measured for both black toner samples as a function of θ . The results are shown in Figure 9.

The solid lines in Fig. 9 were constructed from Fresnel's law for p -polarized light. Fresnel's laws for both s and p directions of linear polarization are summarized in Eqs. (2) and (4), where n_c is the complex index of refraction and is a function of the two optical constants n and κ . These equations are taken as an engineering starting point for the analysis of the data generated with the microgoniophotometer. A description of the origins of these equations and of Fresnel's laws can be found in any good optics text.¹⁰

It is notable that both black toners were well modeled with $\kappa=0$. This is indicated by the experimental values $\rho_p(\theta)=0$ at the angle known as Brewster's angle.¹⁰ As observed for the black and white nylon samples in Table I, specular reflections from the two toner blacks are governed only by their indexes of refraction, n , and not significantly by κ .

$$\varphi(\theta) = \sin^{-1}\left(\frac{\sin(\theta)}{n_c}\right) \quad \text{where } n_c = n(1 - i\kappa), \quad (2)$$

$$\rho_p(\theta) = \frac{\tan[\theta - \varphi(\theta)]\overline{\tan[\theta - \varphi(\theta)]}}{\tan[\theta + \varphi(\theta)]\overline{\tan[\theta + \varphi(\theta)]}}, \quad (3)$$

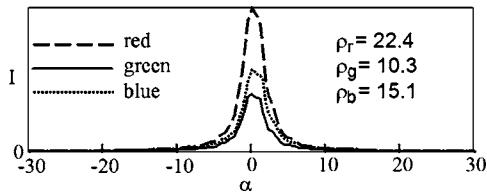


Figure 10. Cyan ink from an ink jet printer measured in red, green, and blue light.

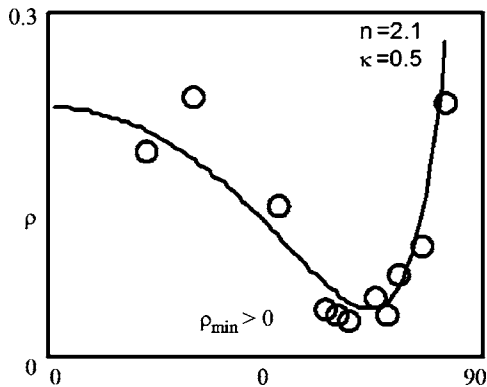


Figure 11. ρ vs θ for the cyan of Fig. 10 measured in red light as a function of θ . Note that $\rho_{\min} > 0$ at Brewster's angle implies $\kappa > 0$.

$$\rho_s(\theta) = \frac{\sin[\theta - \varphi(\theta)] \cdot \overline{\sin[\theta - \varphi(\theta)]}}{\sin[\theta + \varphi(\theta)] \cdot \overline{\sin[\theta + \varphi(\theta)]}}, \quad (4)$$

where the overbar indicates the complex conjugate.

The absorption coefficient, κ , cannot always be ignored in the specular optics of printed images. This is illustrated by the behavior of a cyan patch printed by a commercial ink jet printer. The BRDF measured in white light indicated an anomalously high value for ρ and prompted further measurements in red, green, and blue light. The three BRDF for the cyan sample are shown in Figure 10 along with the three values of ρ .

A previous article on the effect of RGB light on CMY printed samples indicated that the light that is least strongly absorbed shows the greatest reflectance.¹³ This was found to be a result of subsurface specular reflections. Exactly the reverse of this subsurface effect is evident in Fig. 10. The red light is most strongly absorbed by the cyan ink, and it is also the light that undergoes the strongest specular reflection. This behavior can be rationalized if either n or κ is a significant function of the extinction of light, and both effects are well known.¹⁰ To explore this effect in the cyan sample of Fig. 10, measurements of ρ were made in red light as a function of the Fresnel angle, θ . The results are shown in Figure 11 along with Fresnel's law modeled for $\rho_p(\theta)$. The model fits well with the data for $n = 2.1$ and $\kappa = 0.5$, and it is evident that both the increase in n and the significant contribution from κ result from a significant extinction coefficient of the cyan ink with red light.

CONCLUSION

The results of this study show that the microgoniophotometer described in previous reports can be calibrated to absolute reflectance values of known reference materials. By applying the calibrated analysis to printed samples, significantly more information can be obtained than is available through a traditional gloss meter. In particular, the absolute specular reflectance factor of the printed image can be estimated at a two significant figure levels of precision. However, there is some evidence that the analysis may be subject to some experimental artifacts from extreme types of surface microstructure, as for example surfaces produced by sanding.

The analytical technique can be applied at different Fresnel gloss angles, θ , to add additional information about the optical constants n and κ that govern the reflectance factor, ρ . In addition, the analysis can be carried out with different wavelengths of light to explore the spectral and subsurface effects on specular reflectance. In summary, it is now possible to carry out direct experiments to distinguish between all of the factors that govern specular reflectance in a printed sample. These factors have been shown to be: (a) Surface topography, indicated by the shape of the BRDF, (b) the material optical constants, n and κ , and (c) the subsurface reflections, as described in a previous report.¹³

ACKNOWLEDGMENTS

The authors express their thanks to Hewlett-Packard Corporation in Boise, ID, for supporting this work. Thanks also go to Lexmark Corporation in Lexington, KY, for providing some interesting samples to measure.

REFERENCES

- R. S. Hunter and R. W. Harold, *The Measurement of Appearance*, 2nd ed. (Wiley-Interscience, New York, 1987).
- J. S. Arney, L. Ye, E. Maggard, and B. Renstrom, "Gloss granularity of electrophotographic prints", *J. Imaging Sci. Technol.* **51**(4), 293–298 (2007).
- J. S. Arney, K. Pollmeier, and J. Michel, "Technique for analysis of surface topography of photographic prints by spatial analysis of first surface reflectance", *J. Imaging Sci. Technol.* **46**(4), 350 (2002).
- J. S. Arney, P. G. Anderson, and H. Heo, "A microgoniophotometer and the measurement of print gloss", *J. Imaging Sci. Technol.* **48**(5), 458 (2004).
- J. S. Arney and H. Tran, "An inexpensive microgoniophotometry you can build", *Proc. IS&T's PICS Conference* (IS&T, Springfield, VA, 2002) pp. 179–182.
- J. S. Arney, L. Ye, and S. Banach, "Interpretation of gloss meter measurements", *J. Imaging Sci. Technol.* **50**(6), 567 (2006).
- M. A. MacGregor and P. Å. Johansson, "Submillimeter gloss variations in coated paper: Part 1: The gloss imaging equipment and analytical techniques", *Tappi J.* **73**, 161 (1990).
- M.-C. Beland and L. Mattsson, "Optical print quality of coated papers", *J. Pulp Pap. Sci.* **23**(11), 493 (1997).
- P. Å. Johansson, "Optical homogeneity of prints", Ph.D. dissertation, Royal Institute of Technology, Department of Pulp and Paper Chemicals and Technology, Stockholm, Sweden (1999).
- F. A. Jenkins and H. E. White, in *Fundamentals of Optics*, 3rd ed. (McGraw-Hill, New York, 1957), pp. 524 and 1957.
- Angstrom Sun Technologies, Inc. "Online database of optical constants", (<http://www.angstec.com/index.html>), 2007.
- Parker-Textloc Co., Fort Worth, Texas, "Online database of optical constants", (<http://www.texloc.com/closet/cl-refractiveindex.html>), 2007.
- J. S. Arney, P. G. Anderson, G. Franz, and W. Pfeister, "Color properties of specular reflections", *J. Imaging Sci. Technol.* **50**(3), 228 (2006).